The Plant Cell, Vol. 25: 4439–4450, November 2013, www.plantcell.org

Rho of Plant GTPase Signaling Regulates the Behavior of *Arabidopsis* Kinesin-13A to Establish Secondary Cell Wall Patterns[W]

Yoshihisa Oda[a,b,1] and Hiroo Fukuda[a]

[a] Department of Biological Sciences, Graduate School of Science, University of Tokyo, Bunkyo-ku, Tokyo 113-0033, Japan
[b] Precursory Research for Embryonic Science and Technology, Japan Science and Technology Agency, Kawaguchi, Saitama 332-0012, Japan

Plant cortical microtubule arrays determine the cell wall deposition pattern and proper cell shape and function. Although various microtubule-associated proteins regulate the cortical microtubule array, the mechanisms underlying marked rearrangement of cortical microtubules during xylem differentiation are not fully understood. Here, we show that local Rho of Plant (ROP) GTPase signaling targets an *Arabidopsis thaliana* kinesin-13 protein, Kinesin-13A, to cortical microtubules to establish distinct patterns of secondary cell wall formation in xylem cells. Kinesin-13A was preferentially localized with cortical microtubules in secondary cell wall pits, areas where cortical microtubules are depolymerized to prevent cell wall deposition. This localization of Kinesin-13A required the presence of the activated ROP GTPase, MICROTUBULE DEPLETION DOMAIN1 (MIDD1) protein, and cortical microtubules. Knockdown of *Kinesin-13A* resulted in the formation of smaller secondary wall pits, while overexpression of *Kinesin-13A* enlarged their surface area. Kinesin-13A alone could depolymerize microtubules in vitro; however, both MIDD1 and Kinesin-13A were required for the depolymerization of cortical microtubules in vivo. These results indicate that Kinesin-13A regulates the formation of secondary wall pits by promoting cortical microtubule depolymerization via the ROP-MIDD1 pathway.

INTRODUCTION

The plant cell wall plays a central role in cell shaping. Cellulose microfibrils, the major component of the cell wall, constrain cell expansion; therefore, cell shape reflects the pattern of cellulose deposition. Cortical microtubule arrays regulate the cell wall formation pattern by influencing the targeting (Crowell et al., 2009; Gutierrez et al., 2009) and trajectory (Paredez et al., 2006) of the cellulose synthase complex at the plasma membrane. In elongating cells, cortical microtubules are usually arranged in transverse arrays that enable nonisotropic cell growth. This parallel arrangement of cortical microtubules is well characterized and is thought to be self-organized via the dynamic interaction between cortical microtubules (Wasteneys and Ambrose, 2009). The dynamic instability of their plus ends results in casual encounters between cortical microtubules (Shaw et al., 2003); depending on the angle between the encountered microtubules, bundling or catastrophe can occur (Dixit and Cyr, 2004). Cortical microtubules are nucleated from the side of cortical microtubules, thereby forming a branch or a bundle structure (Murata et al., 2005; Chan et al., 2009). Release of nucleated cortical microtubules from the mother microtubule promotes their parallel organization (Nakamura et al., 2010; Lin et al., 2013).

In leaf epidermal pavement cells, interdigitated cell growth is mediated by two Rho of Plant (ROP) GTPase signaling pathways: The ROP6-ROP-INTERACTIVE CRIB MOTIF-CONTAINING PROTEIN1 (RIC1)-katanin pathway promotes ordering of parallel cortical microtubules to maintain indentations, while the ROP2-RIC4 pathway promotes accumulation of actin microfilaments to induce local outgrowth of the cell (Fu et al., 2005, 2009; Lin et al., 2013). These two pathways are spatially coordinated by their mutual inhibition (Fu et al., 2005) and an auxin-mediated feedback loop (Xu et al., 2010). Although ROP GTPase signaling appears to play important roles in cell wall patterning by cortical microtubules, the mechanism underlying local regulation of cortical microtubule dynamics, in particular, that underlying temporal and spatial disassembly of cortical microtubules through ROP GTPase signaling, is largely unknown.

Xylem vessels develop secondary cell walls that are organized into distinct formations, such as annular, spiral, reticulate, and pitted patterns. The secondary cell wall patterns are tightly associated with xylem cell types; metaxylem vessels usually deposit secondary cell walls in reticulate and pitted patterns, while protoxylem vessels deposit secondary cell walls in annular or spiral patterns (Oda and Fukuda, 2012b). Xylem vessels undergo programmed cell death, during which cell contents are lysed to leave thick secondary walls that form a hollow conductive tube (Fukuda, 2000). The secondary cell walls provide physical support to prevent pressure-induced collapse of the vessel (Esau, 1977). Secondary cell wall pits, areas where the secondary cell wall is not deposited, provide a lateral pathway for transporting

[1] Address correspondence to oda@biol.s.u-tokyo.ac.jp.
The authors responsible for distribution of materials integral to the findings presented in this article in accordance with the policy described in the Instructions for Authors (www.plantcell.org) are: Yoshihisa Oda (oda@biol.s.u-tokyo.ac.jp) and Hiroo Fukuda (fukuda@biol.s.u-tokyo.ac.jp).
[W] Online version contains Web-only data.
www.plantcell.org/cgi/doi/10.1105/tpc.113.117853

xylem sap. Cortical microtubules play a central role in secondary cell wall deposition; during xylem vessel differentiation, cortical microtubules are bundled and disassembled at multiple domains to establish the distinct secondary cell wall pattern (Oda et al., 2005, 2010; Oda and Hasezawa, 2006). Although several microtubule-associated proteins (MAPs), including MAP65 (Mao et al., 2006) and MAP70 (Pesquet et al., 2010), regulate the organization of cortical microtubules during xylem differentiation (Oda and Fukuda, 2012b), the overall mechanism underlying the spatial determination of secondary wall deposition in xylem cells has not yet been clarified.

Our previous study using cultured *Arabidopsis thaliana* cells demonstrated that the microtubule-associated MICROTUBULE DEPLETION DOMAIN1 (MIDD1) protein is anchored to plasma membrane domains and causes the formation of secondary cell wall pits (Oda et al., 2010). The plasma membrane domains are established by local activation of the Rho-like GTPase ROP11 by ROPGEF4 and ROPGAP3. Activated ROP11 interacts directly with MIDD1 and anchors it to the plasma membrane domains (Oda and Fukuda, 2012a). Plasma membrane–associated MIDD1 preferentially labels the tips of cortical microtubules during their shrinkage in secondary cell wall pits. Knockdown of MIDD1 prevents local depletion of cortical microtubules and overexpression of MIDD1 reduces their density, suggesting that MIDD1 is an essential component of the microtubule depletion process (Oda et al., 2010). However, MIDD1 is not able to depolymerize microtubules in vitro (Oda et al., 2010), suggesting the involvement of a second protein in this process.

A recent study showed that an *Arabidopsis* kinesin-13 protein, Kinesin-13A, interacts with MIDD1 in yeasts through the C-terminal coiled-coil domain of Kinesin-13A. The authors also showed that they localized along filamentous structures in leaf epidermal cells (Mucha et al., 2010). In animals, members of the kinesin-13 family have microtubule depolymerization activity (Desai et al., 1999; Moores and Milligan, 2006). Although Kinesin-13A is involved in trichome morphogenesis (Lu et al., 2005), its molecular function in plant cells is currently unclear. In this study, we investigated the function of Kinesin-13A in metaxylem vessel cells. Kinesin-13A was preferentially localized to secondary wall pits, and this localization required direct association with MIDD1 and local activation of ROP11. Kinesin-13A displayed microtubule disassembly activity both in vitro and in vivo. The results presented here indicate that Kinesin-13A plays a central role in microtubule disassembly via the active ROP-MIDD1 cascade, which establishes the secondary cell wall pattern in metaxylem vessel cells.

RESULTS

Localization of Kinesin-13A in Differentiating Xylem Cells

To examine the subcellular localization of Kinesin-13A in differentiating xylem cells, p*Kinesin-13A*:*GFP-Kinesin-13A* was introduced into cultured *Arabidopsis* cells harboring inducible *VASCULAR-RELATED NO APICAL MERISTEM/ARABIDOPSIS TRANSCRIPTION ACTIVATION FACTOR/CUP-SHAPED COTYLEDON-DOMAIN6* (*VND6*), which promotes metaxylem vessel cell differentiation (Oda et al., 2010). Punctuated green fluorescent protein (GFP) signals were detected preferentially in the secondary cell wall pits of differentiating metaxylem vessel cells (Figures 1A and 1B; see Supplemental Movie 1 online). A

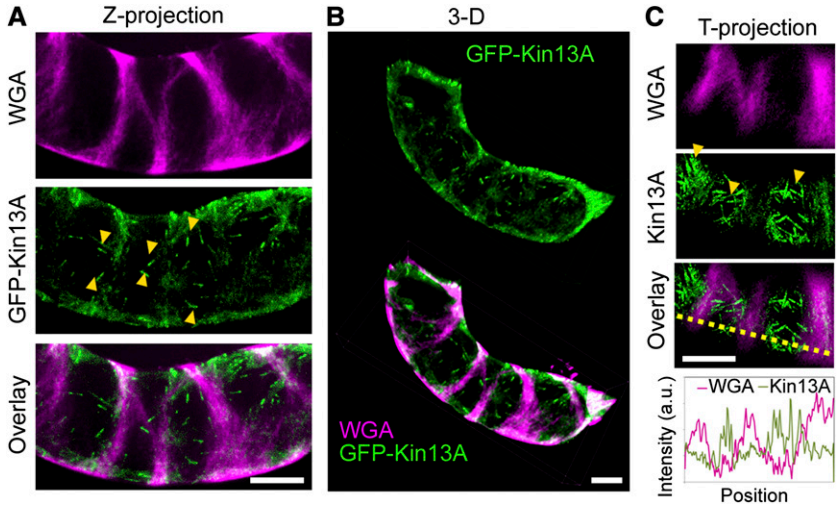

Figure 1. Kinesin-13A Is Localized to Secondary Cell Wall Pits.

(A) Localization of GFP-Kinesin-13A (GFP-Kin13A) and secondary cell walls labeled with fluorescent WGA. Arrowheads indicate preferential localization of GFP-Kinesin-13A in the secondary cell wall pits.

(B) Three-dimensional re-construction of the cell shown in **(A)**.

(C) Projection of time-lapse images of GFP-Kinesin-13A and WGA-labeled secondary cell walls. Arrowheads indicate preferential localization of GFP-Kinesin-13A in the secondary cell wall pits. The graph in the bottom panel shows the intensity profile along the dotted yellow line. a.u., arbitrary units. Bars = 5 μm.

projection of time-lapse images with intensity profiling confirmed the accumulation of Kinesin-13A in secondary cell wall pits (Figure 1C). Double labeling experiments and projection of time-lapse images revealed that Kinesin-13A colocalized with cortical microtubules in these regions (Figures 2A and 2B). A kymograph analysis, in which the behavior of Kinesin-13A along the microtubule over time is sequentially displayed side-by-side, revealed that Kinesin-13A was associated with microtubules in secondary wall pits (Figures 2C and 2D).

The localization and dynamics of Kinesin-13A identified here are similar to those of MIDD1 (Oda et al., 2010); therefore, the interaction between these proteins was examined. Cointroduction of Kinesin-13A and MIDD1 into *Arabidopsis* cells caused depolymerization of microtubules (see below); therefore, we used a truncated Kinsein-13A (Kinsein-13A$^{\Delta M}$) that lacked the N-terminal region containing the motor domain but included the C-terminal MIDD1-interacting coiled-coil domain (Mucha et al., 2010). As expected, MIDD1 and Kinesin-13A$^{\Delta M}$ colocalized in the membrane domains underlying secondary cell wall pits (Figure 3A). To determine whether Kinesin-13A interacts with MIDD1 directly in these regions, a bimolecular fluorescence complementation (BiFC) assay was used. MIDD1 and Kinesein-13A$^{\Delta M}$ were fused with the C-terminal (cYFP) and N-terminal (nYFP) regions of yellow fluorescent protein, respectively, and then expressed in the leaf epidermis of *Nicotiana benthamiana*. No fluorescent signals were detected following expression of either construct alone, but a strong signal was generated following coexpression of cYFP-MIDD1 and nYFP-Kinesein-13A$^{\Delta M}$, indicating that Kinesin-13A interacts with MIDD1 in vivo (Figure 3B). When these constructs were introduced into inducible *Arabidopsis* xylem cells, the YFP fluorescent signal did not overlap with that of wheat germ agglutinin (WGA)–labeled secondary cell walls, indicating that Kinesin-13A interacts directly with MIDD1 in secondary cell wall pits (Figure 3C). We next examined the MIDD1 dependency of Kinesin-13A localization. GFP-Kinesin-13A$^{\Delta M}$ was localized to the cytoplasm in 43 of 49 *MIDD*-knockdown (*midd1-kd*) cells (Oda et al., 2010), while it localized to filamentous structures, which are microtubules, in 30 of 34 control cells (Figure 3D). The remaining six cells showed the localization along microtubules as observed in control cells. This suggests that the localization of Kinesin-13A along microtubules in secondary cell wall pits is dependent upon MIDD1. On the other hand, in cells coexpressing tagRED FLUORESCENT PROTEIN (tagRFP)-ROP11^{Q66L}, a constitutively active form of ROP11 that induces broad activation of ROP11, which causes the microtubule localization of MIDD1 broadly (Oda and Fukuda,

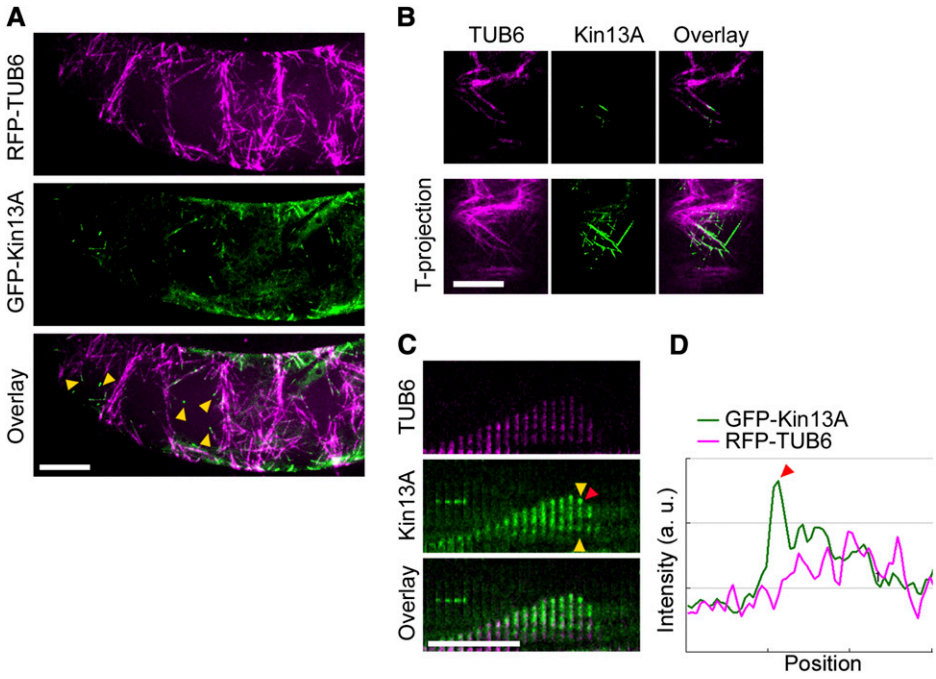

Figure 2. Kinesin-13A Colocalizes with Cortical Microtubules in Secondary Wall Pits.

(A) Localization of microtubules (tagRFP-TUB6) and GFP-Kinesin-13A (GFP-Kin13A) in differentiating xylem cells. Arrowheads indicate preferential localization of GFP-Kinesin-13A along cortical microtubules in secondary cell wall pits.

(B) Projection of time-lapse images of GFP-Kinesin-13A and tagRFP-TUB6. Kinesin-13A colocalizes with microtubules.

(C) Kymograph of tagRFP-TUB6 and GFP-Kinesin-13A. The yellow arrowheads indicate the section used to generate the intensity profile shown in **(D)**. The red arrowhead indicates accumulation of Kinesin-13A on the microtubule.

(D) The intensity profile along the section indicated by the yellow arrowheads in **(C)**. a.u., arbitrary units.

Bars = 5 μm.

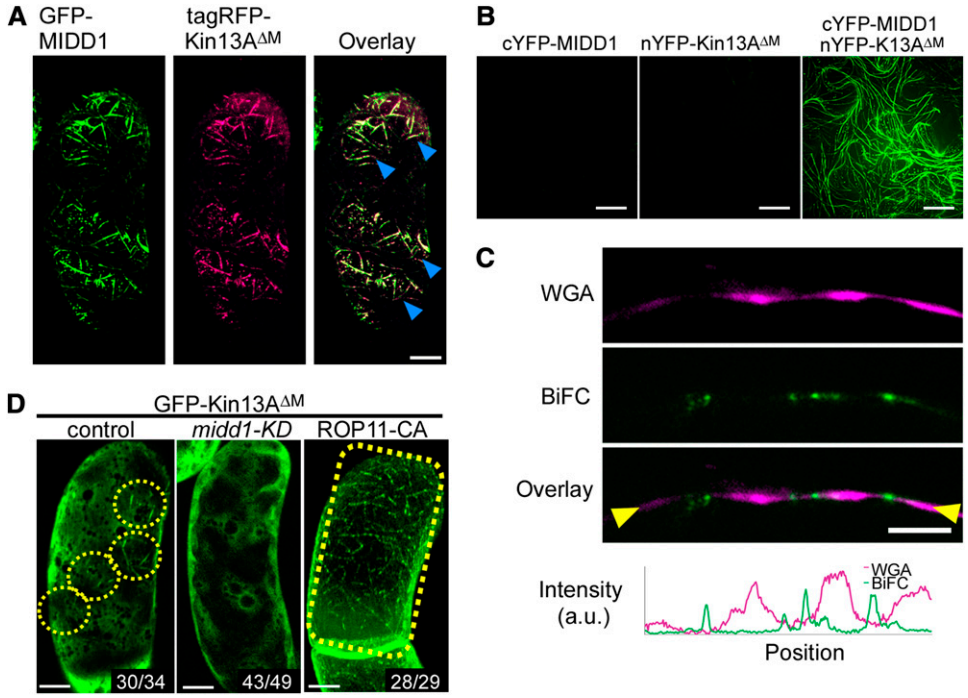

Figure 3. Kinesin-13A Is a Component of the ROP11-MIDD1 Complex.

(A) Localization of GFP-MIDD1 and tagRFP-Kinesin-13A$^{\Delta M}$ (tagRFP-Kin13A$^{\Delta M}$) in a differentiating xylem cell. Arrowheads indicate colocalization of the two proteins.

(B) Results of a BiFC assay of the leaf epidermis of *N. benthamiana* expressing MDD1 and Kinesin-13A fused with C-terminal half and N-terminal half of YFP, respectively. Note that fluorescence was only detected when cYFP-MIDD1 and nYFP-Kinesin-13A$^{\Delta M}$ were coexpressed.

(C) Results of the BiFC assay in a differentiating xylem cell. The secondary cell wall was labeled with fluorescent WGA. The graph in the bottom panel shows the intensity profile in the region between the yellow arrows. Note that the YFP fluorescent signal was detected in the secondary cell wall pits. a.u., arbitrary units.

(D) Localization of GFP-Kinesin-13A$^{\Delta M}$ in differentiating xylem cells. The yellow dotted areas indicate domains where Kinesin-13A$^{\Delta M}$ was associated with microtubules. Knockdown of *MIDD1* (*midd1-KD*) abolished the localization of Kinesin-13A$^{\Delta M}$ to cortical microtubules, and coexpression of constitutively active ROP11 (ROP11-CA) promoted this localization. The number of cells with similar Kinesin-13A$^{\Delta M}$ localization is indicated at each panel.

Bars = 5 μm.

2012a), Kinesein-13A$^{\Delta M}$ was broadly localized to microtubules in 28 of 29 observed cells (Figure 3D). These results suggest that Kinesin-13A is associated with the active ROP-MIDD1 complex.

Function of Kinesin-13A in Vivo

To examine the role of Kinesin-13A in secondary cell wall formation, *Kinesin-13A* was knocked down by RNA interference. We introduced *35S*:*Kinesin-13A-RNA interference* (*RNAi*)/*LexA*:*GFP* into VND6-inducible cultured cells; this construct contains an inverted repeat of the *Kinesin-13A* fragment and an additional GFP expression cassette that enables identification of transformed cells without cell selection using antibiotics. We used *35S*:β-*glucuronidase* (*GUS*)-*RNAi*/*LexA*:*GFP* as a control. GFP-positive cells were collected by fluorescence-activated cell sorting, and *Kinesin-13A* mRNA levels were measured by quantitative RT-PCR. *Kinesin-13A* mRNA levels were similar in GFP-positive and GFP-negative cells from the *35S*:*GUS-RNAi*/*LexA*:*GFP*–introduced culture; however, in the *35S*:*Kinesin-13A-RNAi*/*LexA*:*GFP*–introduced culture, the *Kinesin-13A* mRNA levels in GFP-positive cells were significantly lower than those in GFP-negative cells (Figure 4A). In accordance with the reduced levels of *Kinesin-13A* mRNA, *Kinesin-13A*–knockdown cells showed smaller secondary cell wall pits than control cells (Figures 4B and 4C). Similarly, an *Arabidopsis* line (SALK_104697) in which T-DNA was inserted into an exon of the *Kinesin-13A* gene (designated *kinesin-13a*) (Figures 4D and 4E) had undetectable levels of Kinsein-13A and smaller pits in the secondary cell walls of root metaxylem vessels than wild-type plants (Figures 4F and 4G). Introduction of *pKinesin-13A*:*GFP-Kinesin-13A* complemented the phenotype of reduced pit size, confirming the role of *Kinesin-13A* in secondary cell wall pit expansion. However, GFP fluorescence was not detected clearly in the complemented plants, probably as a result of low expression level of *Kinesin-13A*.

We also examined the effect of Kinesin-13A overexpression on secondary cell wall pit size. When Kinesin-13A expression

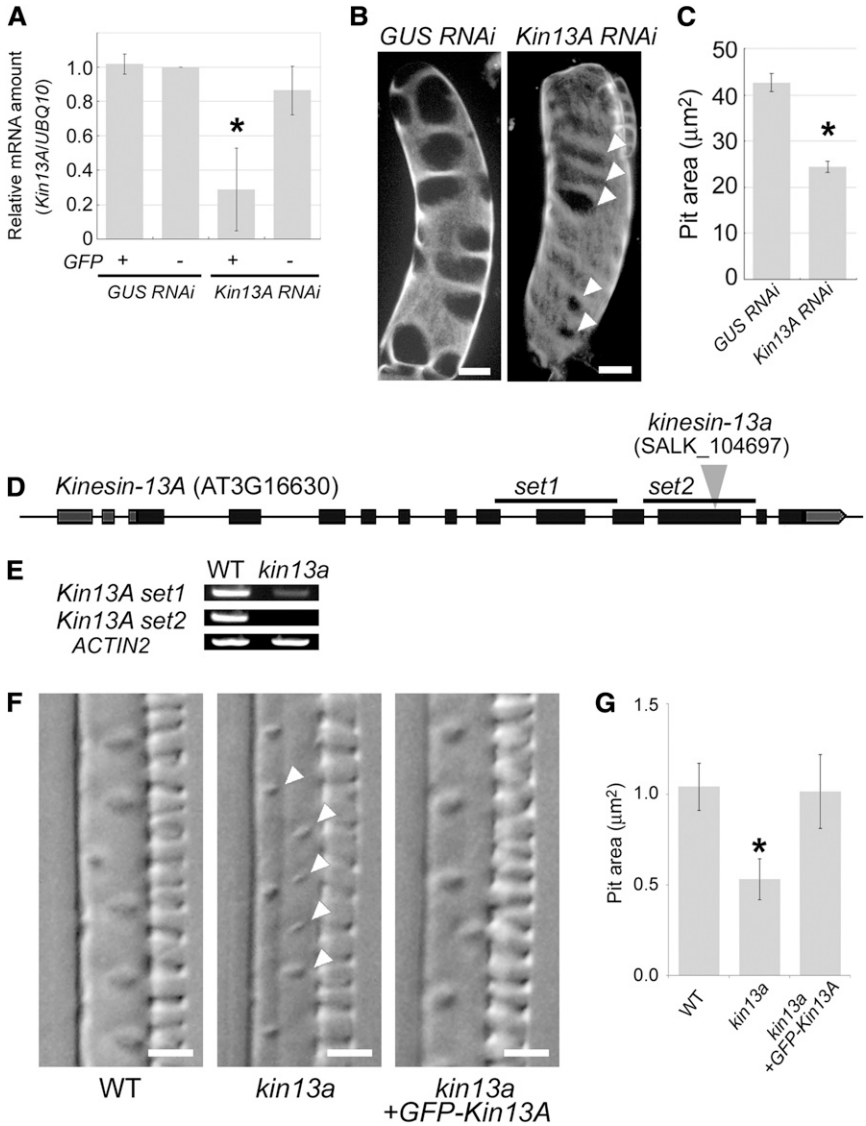

Figure 4. Kinesin-13A Is Required for Extension of Secondary Cell Wall Pits.

(A) Quantitative RT-PCR analysis of *Kinesin-13A* mRNA levels in GFP-positive and GFP-negative *Kinesin-13A-RNAi* and *GUS-RNAi* lines. Data represent the mean ± SD (n = 3). *P < 0.01; ANOVA with Scheffe's test.

(B) Secondary cell wall patterns formed in *Kinesin-13A-RNAi* (*Kin13A* RNAi) and *GUS-RNAi* control cells. The arrowheads indicate small pits in secondary cell walls. Bars = 5 μm

(C) The surface area of secondary cell wall pits in *Kinesin-13A-RNAi* and *GUS-RNAi* cells. Data represent the mean ± SD (n > 200 pits). *P < 0.01; Student's t test.

(D) Schematic illustration of the loss-of-function mutants of *Kinesin-13A*. T-DNA was inserted into an exon of the *Kinesin-13A* gene in the *kinesin-13a* line. Set1 and set2 indicate regions used for RT-PCR shown in **(E)**.

(E) RT-PCR analysis of *Kinesin-13A* mRNA in wild-type (WT) and *kinesin-13a*-lines.

(F) Metaxylem vessel cells in roots in wild-type, *kinesin-13a*, and complemented plants expressing GFP-Kinesin-13A. The arrowheads indicate small pits in secondary cell walls. Bars = 5 μm.

(G) The surface area of secondary cell wall pits in wild-type, *kinesin-13a*, and complemented plants expressing GFP-Kinesin-13A. Data represent the mean ± SD of 12 plants (n > 100 pits). *P < 0.01; ANOVA with Scheffe's test.

was induced by treating *Arabidopsis* plants harboring *LexA*:*GFP-Kinesin-13A* with 2 μM estradiol for 2 d, the root metaxylem vessels produced abnormally large secondary cell wall pits and protoxylem vessels exhibited slightly wider secondary cell wall bundles than wild-type protoxylem vessels (Figure 5A). To examine cortical microtubule organization in cells overexpressing Kinesin-13A in vivo, *LexA*:*GFP-Kinesin-13A* was introduced into plants harboring *35S*:*tagRFP-TUB6* (for β-*6 TUBULIN*). The parallel cortical microtubules in root epidermal cells were completely disrupted 24 h after the induction of

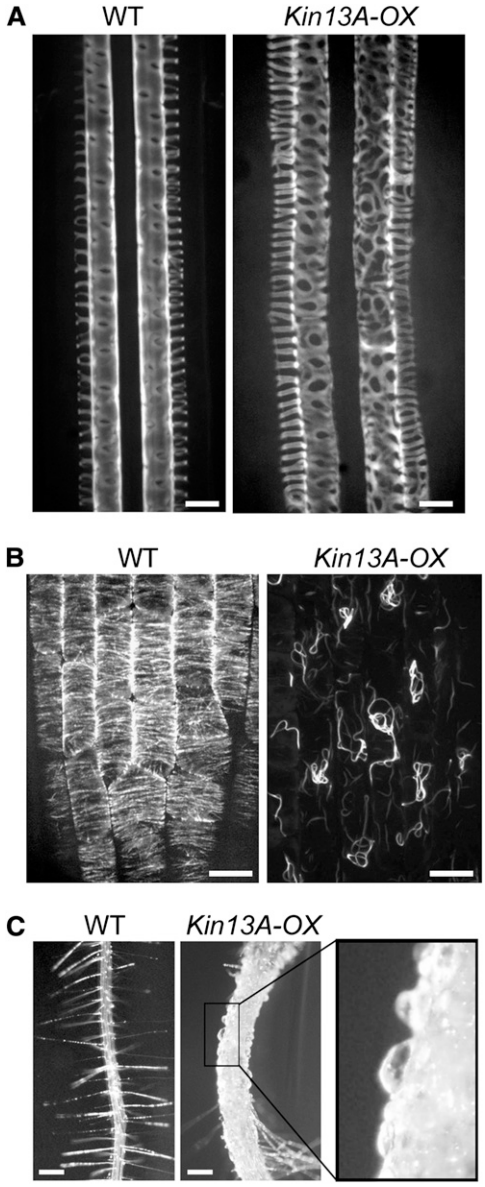

Figure 5. Overexpression of *Kinesin-13A* Induces Microtubule Disruption and Enlarged Secondary Wall Pits.

(A) to **(C)** The phenotypes of wild-type (WT) plants and plants overexpressing *GFP-Kinesin-13A* (*Kin13A-OX*) after treatment with 2 μm estradiol.
(A) The secondary cell wall pattern of xylem vessels stained with Safranin-O 2 d after induction.
(B) Cortical microtubules (*35S*:*tagRFP-TUB6*) in the root cortex 24 h after induction of GFP-Kinesin-13A expression.
(C) Roots 2 d after induction of GFP-Kinesin-13A.
Bars = 10 μm in **(A)** and **(B)** and 100 μm in **(C)**.

GFP-Kinesin-13A (Figure 5B). Consistent with this, long-term expression of GFP-Kinesin-13A caused the roots to swell (Figure 5C) as a result of microtubule disruption. These results suggest that Kinesin-13A enlarges secondary cell wall pits through microtubule disassembly.

Kinesin-13A Induces Microtubule Disassembly in Vitro

To determine whether Kinesin-13A shows microtubule depolymerizing activity, an in vitro microtubule depolymerization assay (Desai et al., 1999) was performed. Glutathione *S*-transferase (GST)–tagged Kinesein-13A and MIDD1 were overexpressed in *Escherichia coli* and then purified. As a positive control, GST-hsKif2A, a human kinesin-13 protein that can induce microtubule disassembly (Noda et al., 2012), was also prepared. The purified GST-tagged proteins were incubated with taxol-stabilized microtubules containing fluorescein-tagged tubulin in a buffer supplemented with ATP or adenylyl imidodiphosphate (AMPPNP), a nonhydrolyzable analog of ATP. Microtubule depolymerization was then observed under a fluorescence microscope. In the presence of ATP, both GST-hsKif2A and GST-Kinesin-13A disrupted microtubules, while GST-MIDD1 did not; however, in the presence of AMPPNP, GST-Kinesin-13A could not induce depolymerization (Figure 6A).

Microtubule depolymerization was then examined further using biochemical methods. The samples were ultracentrifuged and then separated by SDS-PAGE; in this experiment, the supernatant and pellet fractions represented tubulin dimers and microtubule polymers, respectively. In the presence of ATP, the addition of GST-hsKif2A or GST-Kinesin-13A markedly increased the amount of tubulin in the supernatant and decreased the amount of tubulin in the microtubule pellet (Figure 6B). These effects were not seen when ATP was replaced with AMPPNP (Figure 6B), indicating that GST-Kinesin-13A possesses ATP-dependent microtubule depolymerization activity.

Kinesin-13A Requires MIDD1 for the Depolymerization of Cortical Microtubules in Vivo

Although our experiments revealed that Kinsein-13A promotes microtubule depolymerization both in vitro and in vivo, previous articles reported that Kinesin-13A does not localize to cortical microtubules (Lu et al., 2005; Wei et al., 2009). We hypothesized that this apparent discrepancy is attributable to the absence or presence of MIDD1, which may contribute to the targeting of Kinesin-13a to microtubules in vivo. To investigate this hypothesis, the localization of Kinesin-13A and cortical microtubule density were examined by introducing *LexA*:*tagRFP-Kinesin-13A* and *35S*:*GFP-TUB6* into an *Arabidopsis* nonxylem cell line, which does not express MIDD1 (Oda et al., 2010). Kinesin-13A was not localized to cortical microtubules and did not induce cortical microtubule depolymerization in nonxylem cells (Figures 7A and 7E). Instead, Kinesin-13A was localized to punctate structures, which is consistent with previous reports (Lu et al., 2005; Wei et al., 2009). By contrast, Kinesin-13A$^{\Delta M}$ was localized to the cytoplasm (Figure 7B). Next, to enable coexpression of MIDD1 and Kinesin-13A, *LexA*:*tagRFP-Kinesin-13A* was introduced into a newly established stable transgenic cell line harboring *LexA*:*MIDD1.* Coexpression of tagRFP-Kinesin-13A and MIDD1 led to a marked reduction in the number of cortical microtubules (Figures 7C and 7E), indicating that Kinesin-13A requires MIDD1 to depolymerize microtubules in vivo. Induction of MIDD1 shifted the localization of Kinesin-13A$^{\Delta M}$ from the cytoplasm (Figure 7B) to the cortical

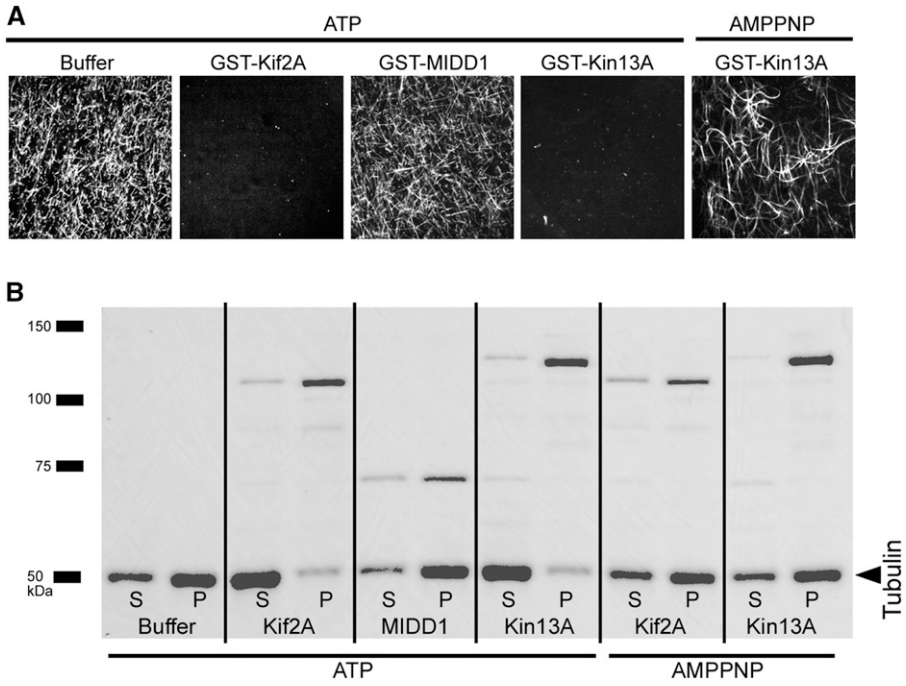

Figure 6. Kinesin-13A Induces Microtubule Disassembly in Vitro but MIDD1 Does Not.

(A) Visualization of microtubule depolymerization by fluorescence microscopy. Taxol-stabilized microtubules containing fluorescein-tagged tubulin were incubated with GST-hsKif2A, GST-MIDD1, or GST-Kinesin-13A (GST-Kin13A) in control buffer or buffer supplemented with ATP or AMPPNP.
(B) Sedimentation analysis of taxol-stabilized microtubule depolymerization. The indicated reactions were sedimented by ultracentrifugation, and the supernatant (S) and pellet (P) were analyzed by SDS-PAGE. GST-hsKif2A and GST-Kinesin-13A increased the amount of tubulin in the supernatant, whereas GST-MIDD1 did not.

microtubules (Figure 7D). Although coexpression of GFP-MIDD1 and tagRFP-Kinesin-13A caused loss of cortical microtubules, these proteins were completely colocalized in structures reminiscent of aggregated microtubules (Figure 8A). Coexpression of GFP-MIDD1 and tagRFP-Kinesin-13A$^{\Delta M}$ did not affect cortical microtubules, but these two proteins were also colocalized along cortical microtubules (Figure 8B). These results suggest that MIDD1 targets Kinesin-13A to cortical microtubules and is therefore required for its microtubule depolymerization activity.

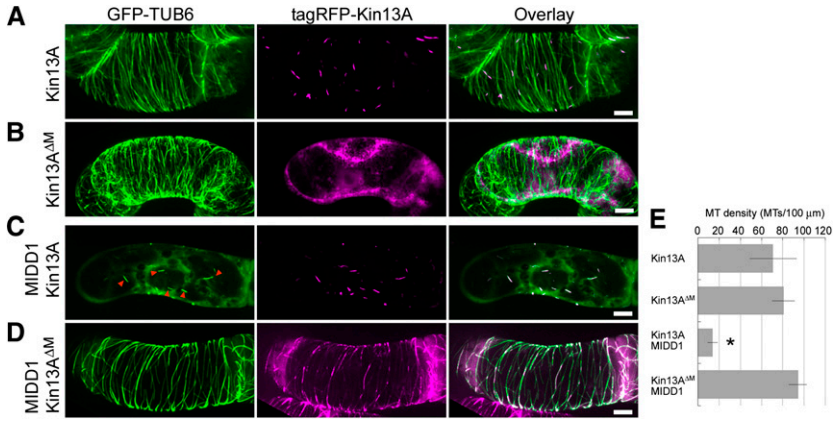

Figure 7. MIDD1 Is Required for Microtubule Disassembly by Kinesin-13A in Nonxylem Cultured Cells.

(A) and **(B)** tagRFP-Kinesin-13A (**[A]**; Kin13A) or tagRFP-Kinesin-13A$^{\Delta M}$ (**[B]**; Kin13A$^{\Delta M}$) were coexpressed with GFP-TUB6 in nonxylem cells.
(C) and **(D)** tagRFP-Kinesin-13A **(C)** or tagRFP-Kinesin-13A$^{\Delta M}$ **(D)** were coexpressed with MIDD1 and GFP-TUB6 in nonxylem, MIDD1-inducible cells. Bars = 5 μm.
(E) The densities of cortical microtubules (MT) in cells expressing the indicated proteins. Red arrowheads indicate disrupted cortical microtubules. Data represent the mean ± SD (n > 100 cells). *P < 0.01; ANOVA with Scheffe's test.

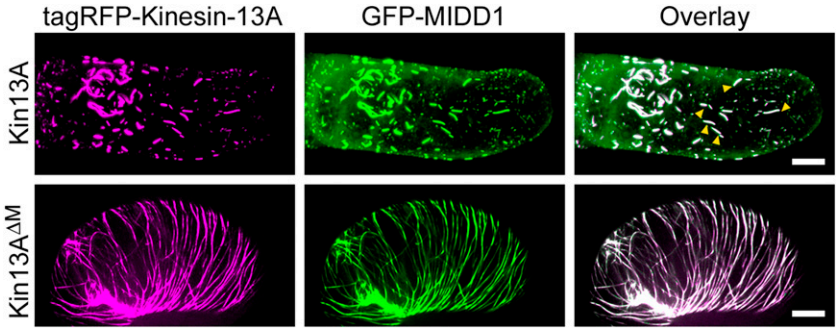

Figure 8. Kinesin-13A Colocalizes with MIDD1 in Nonxylem Cultured Cells.

tagRFP-Kinesin-13A (Kin13A) or tagRFP-Kinesin-13A$^{\Delta M}$ (Kin13A$^{\Delta M}$) was coexpressed with GFP-MIDD1 in nonxylem cells. Both Kinesin-13A and Kinesin-13A$^{\Delta M}$ colocalized with MIDD1. Note that coexpression of full-length Kineisn-13A and MIDD1 caused complete disruption of cortical microtubules. Bars = 5 μm.

DISCUSSION

Kinesin-13A Depolymerizes Microtubules in Plants

Animal kinesin-13 family members are microtubule depolymerizing proteins (Desai et al., 1999; Moores and Milligan, 2006) that play important roles in regulating various microtubule events, including spindle assembly, kinetochore microtubule dynamics (Ems-McClung and Walczak, 2010), neural development (Homma et al., 2003), interphase microtubule dynamics (Mennella et al., 2005), and flagella assembly (Piao et al., 2009). The *Arabidopsis* genome contains two kinesin-13 genes, namely, *Kinesin-13A* and *Kinesin-13B* (Lee and Liu, 2004). Although the cellular localization and roles of *Kinesin-13A* during trichome morphogenesis have been reported (Lu et al., 2005), the molecular function of plant kinesin-13 proteins remains unclear. This study demonstrates that Kinesin-13A shows microtubule depolymerization activity both in vivo and in vitro. The in vitro assay performed here revealed that recombinant Kinesin-13A can depolymerize taxol-stabilized microtubules in an ATP-dependent manner. Conditional overexpression of Kinesin-13A caused the loss of cortical microtubules, which in turn caused the cells in *Arabidopsis* roots to swell.

Arabidopsis microtubule-associated proteins MAP18 and MDP40 inhibit microtubule polymerization, thereby causing destabilization. Overexpression and knockdown of MAP18 or MDP40 induce hypersensitivity and resistance to microtubule depolymerizing drugs, respectively, and also induce changes in cortical microtubule arrays and abnormal cell shape (Wang et al., 2007, 2012). Therefore, MAP18 and MDP40 are considered to be microtubule destabilizing proteins. The katanin-like protein KTN1 is also a regulator of microtubule stability in plants. Overexpression of KTN1 induces microtubule severing that finally results in depolymerization of cortical microtubules (Stoppin-Mellet et al., 2006). The major function of KTN1 is thought to be the ordering of parallel cortical microtubules by cutting off those that are branched from the side of another cortical microtubule (Nakamura et al., 2010; Lin et al., 2013). In summary, various microtubule regulators are involved in microtubule stability in plants; however, knowledge of the way in which plant proteins affect microtubule dynamics is more limited than that of animal proteins. Here, we demonstrated that Kinesin-13A directly depolymerizes microtubules and is therefore a crucial regulator for cortical microtubule dynamics.

The ROP11-MIDD1-Cascade Regulates Kinesin-13A Localization

This study examined the spatial regulation of Kinesin-13A using an *Arabidopsis* xylem cell culture. Live imaging of differentiating xylem cells indicated that Kinesin-13A preferentially localizes with cortical

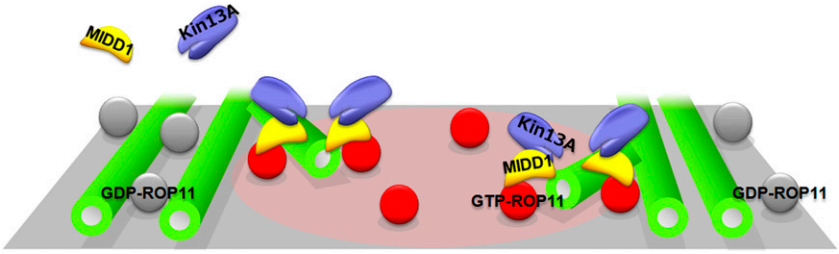

Figure 9. A Schematic Illustration of ROP11-MIDD1-Kinesin-13A Complex in Differentiating Xylem Cells.

Activated ROP11 (GTP-ROP11) recruits MIDD1 to the plasma membrane in future secondary wall pits. MIDD1 directly binds cortical microtubules growing into the future pit region and recruit Kinesin-13A (Kin13A), which then induces depolymerization of the cortical microtubules. Inactive ROP11 (GDP-ROP11) around the future pit region cannot recruit MIDD1; therefore, Kinesin-13A is not targeted to the cortical microtubules.

microtubules in secondary cell wall pits. A BiFC assay suggested that Kinesin-13A also directly associates with MIDD1 in these regions. Knockdown of *MIDD1* abolished the microtubule localization of Kinesin-13A. Because MIDD1 binds to microtubules via its N-terminal domain (Oda et al., 2010), these results suggest that Kinesin-13A binds to microtubules only in the presence of MIDD1. In support of this theory, Kinesin-13A did not colocalize with microtubules in nonxylem-cultured cells that do not express MIDD1, and the introduction of exogenous MIDD1 caused Kinesin-13A to colocalize with microtubules. Based on these results, we conclude that MIDD1 targets Kinesin-13A to microtubules. In the case of Kinesin-13A overexpression in roots, Kinesin-13A might depolymerize microtubules by interacting with endogenous MIDD1.

Introduction of constitutively active ROP11 enhanced the localization of Kinesin-13A along microtubules, indicating that its microtubule targeting is regulated by active ROP. We recently reported that active ROP11 directly recruits MIDD1 to the plasma membrane at regions where secondary cell wall pits are formed (Oda et al., 2010; Oda and Fukuda, 2012a). ROP GUANINE NUCLEOTIDE EXCHANGE FACTOR4 (ROPGEF4) and ROP GTPASE ACTIVATING PROTEIN3 (ROPGAP3) mediate local activation of ROP11, which in turn recruits MIDD1. The localized MIDD1 then promotes cortical microtubule depolymerization to form secondary cell wall–depleted areas. Taken together with the observation that Kinesin-13A shows microtubule depolymerizing activity but MIDD1 does not, it is likely that Kinsein-13A is a functional component of the ROP11-MIDD1 complex that acts to form local cell wall pits (Figure 9). This idea is also supported by our finding that decreases and increases in *Kinesin-13A* expression resulted in the formation of smaller and larger pits, respectively.

Local depletion of cortical microtubules occurs not only in xylem cells but also in various other cells. Cortical microtubules are sparse in the lobes of leaf epidermal cells (Fu et al., 2005) and are absent in the apex of growing pollen tubes (Yang, 2008) and root hairs (Van Bruaene et al., 2004). At the pollen tube apex, ROP GTPases are activated, and ROP INTERACTIVE PARTNER1 (RIP1)/INTERACTOR OF CONSTITUTIVE ACTIVE ROPS1 (ICR1), which belongs to the same family as MIDD1, is also localized (Li et al., 2008). On the other hand, *Kinesin-13A* is ubiquitously expressed (Winter et al., 2007). Therefore, GTPase signaling might regulate local microtubule depletion via its effects on Kinesin-13A function. In leaf epidermal cells, ROP2-RIC4 signaling promotes accumulation of cortical actin microfilaments in lobes, which eliminates cortical microtubules from the lobe forming regions (Fu et al., 2005). ROP-Kinesin-13A signaling might coordinate with ROP2-RIC4 pathway to eliminate cortical microtubules by inducing microtubule disassembly. Further analyses are required to elucidate whether local depletion of cortical microtubules in various plant cells is generally regulated by the ROP-MIDD/ICR/RIP family member Kinesin-13A.

Plant-Specific Regulation of Kinesin-13A

MIDD1 was required for specific targeting of Kinesin-13A and its microtubule depolymerizing activity in vivo. In animal cells, kinesin-13 proteins directly bind to and depolymerize microtubules without the support of additional proteins such as MIDD1 (Maney et al., 2001; Ovechkina et al., 2002). This *Arabidopsis*-specific requirement for MIDD1 may result from the lack of a neck region within Kinesin-13A, which is conserved between animal kinesin-13 family members. The conserved neck region contains positively charged amino acids that act at the interaction with the microtubule lattice (Ovechkina et al., 2002). Phosphorylation of animal kinesin-13 inhibits or moderates its localization and microtubule depolymerizing activity (Ems-McClung and Walczak, 2010). Therefore, phosphorylation might affect the localization and/or function of Kinesin-13A, resulting in differential requirements for MIDD1 in vivo and in vitro. In any case, a plant-specific protein, MIDD1, functions in enhancing the accessibility of Kinesin-13A to cortical microtubules, supporting local microtubule depolymerization.

In animal cells, various binding partners regulate the localization and activity of kinesin-13 proteins (Ems-McClung and Walczak, 2010; Welburn and Cheeseman, 2012). Most of these binding partners target kinesin-13 proteins to the centrosome and kinetochore to form spindles, whereas others regulate interphase cytoplasmic microtubules. Evidence of Rho GTPase signaling that associates kinesin-13 proteins with the plasma membrane has not been reported in mammals. Plant cortical microtubules develop without centrosomes and are closely associated with the plasma membrane; this acentrosomal microtubule structure is highly unique to plant cells. Considering that ROP GTPases are tightly associated with the plasma membrane and that MIDD1 is a plant-specific scaffold protein that links ROP GTPases to cortical microtubules, the ROP-MIDD1-Kinesin-13A complex may be a crucial plant-specific system that regulates the local depolymerization of cortical microtubules at the plasma membrane. ROP GTPases also interact with another plant-specific scaffold protein, RIC1, which promotes microtubule severing activity of the katanin enzyme to facilitate parallel ordering of cortical microtubules (Lin et al., 2013). By collaborating with this parallel pathway, the ROP-MIDD1-Kinesin-13A complex may eventually determine the shape and function of plant cells.

METHODS

Cell Culture

Arabidopsis thaliana Columbia-0 suspension cells and its derivative strains, the *VND6*-inducible line (Oda et al., 2010) and *VND6*-inducible/*MIDD1*-RNAi line (Oda et al., 2010), were cultured as described previously (Oda and Fukuda, 2011), with a slight modification. Briefly, cells were cultured in modified Murashige and Skoog (MS) medium containing 4.33 g/L MS inorganic salts (Wako Chemicals), 3% Suc, 1 mg/L 2,4-D, and B5 vitamins including 4 mg/L of nicotinic acid, 4 mg/L of pyridoxine-HCl, 40 mg/L of thiamine-HCl, and 400 mg/L of myoinositol, pH 5.8. Transformation of the cells was performed as described previously (Oda and Fukuda, 2011). For stable transformation of *LexA:MIDD1*, 3-d-old cells were cocultured with *Agrobacterium tumefaciens* harboring *LexA:MIDD1* for 48 h in MS medium supplemented with 50 mg/L of acetosyringone. Claforan (0.5 mg/L; Aventis) was added to the culture, and the suspension cells were cultured for a further 5 d. Then, the cells were cultured in the MS medium supplemented with 10 mg/L of hygromycin B. Surviving cells were subcultured every week with hygromycin B at increasing concentrations up to 50 mg/L. Xylem differentiation was induced as described previously (Oda et al., 2010).

Plasmid Construction

To generate *LexA*:*GFP-Kinesin-13A*, *LexA*:*tagRFP-Kinesin-13A*, *LexA*:*GFP-Kinesin-13A*$^{\Delta M}$, and *LexA*:*tagRFP-Kinesin-13A*$^{\Delta M}$, the full-length coding region of *Kinesin-13A* (AT3G16630) or the C-terminal fragment comprising residues 1636 to the stop codon was PCR amplified with appropriate primers (see Supplemental Table 1 online) and cloned into the pENTR/D-TOPO entry vector (Invitrogen). These clones were recombined with pER-GX and pER-RX vectors (Oda and Fukuda, 2012a) using LR clonase mix II (Invitrogen), which resulted in the formation of N-terminal *GFP* and *tagRFP* fusions, respectively. To generate *pKinesin-13A*:*GFP-Kinsein-13A*, a 2-kb region of the promoter of *Kinesin-13A* and *GFP-Kinesin-13A* was amplified and fused by PCR. The fused fragment was cloned into the pEntr/D-TOPO vector, which was then recombined with the pGWB501 vector (Nakagawa et al., 2007).

For the *Kinesin-13A* RNAi experiments, the first 400 bp of the *Kinesin-13A* coding sequence and an intron of *WRKY33* were amplified and fused by PCR. The fused sequence was then cloned into the pEntr/D-TOPO vector. The reverse-orientation 400-bp fragment of the *Kinesin-13A* coding sequence was inserted into the 3′ end of the *WRKY* 33 intron using an In-Fusion HD cloning kit (Clontech). This inverted repeat was recombined with the pMDC7 vector using an LR reaction. For *35S:Kinesin-13A-RNAi/LexA*:*GFP*, the Nos terminator-LexA fragment was PCR amplified from a pER8 vector with additional *Asc*I sites at the 5′ and 3′ end and then inserted into the *Asc*I site of the pEntr vector harboring the inverted repeat of *Kinesin-13A*.

To generate the constructs used in the BiFC assay, a DNA sequence encoding residues 1 to 172 of enhanced YFP was inserted at the *Not*I site of the pEntr/D-TOPO vector harboring *Kinesin-13A*$^{\Delta M}$. Another DNA fragment encoding residues 158 to 240 of enhanced YFP was inserted to the *Not*I site of the pEntr/D-TOPO vector harboring the *MIDD1*$^{\Delta N}$ coding sequence. These vectors were then recombined with the pMDC7 vector.

Microscopy

Cells were observed under an inverted fluorescence microscope fitted with a confocal unit as described previously (Oda et al., 2010). A second system comprising an inverted microscope (IX83-ZDC; Olympus), a confocal unit (CSU-W1; Yokogawa), a cooled charge-coupled device camera (ORCA-R2; Hamamatsu Photonics), and laser lines set at 488 and 561 nm was also used. Kymograph analysis was performed using Image J software (http://rsbweb.nih.gov/ij/).

Transient Expression in *Nicotiana benthamiana*

Transient expression in *N. benthamiana* was performed as described previously (Oda and Fukuda, 2012a).

Protoplast and Fluorescence-Activated Cell Sorting

Cell sorting was performed as described previously (Birnbaum et al., 2005), with a few modifications. Cultured *Arabidopsis* cells were suspended in enzyme solution containing 600 mM mannitol, 2 mM $MgCl_2$, 0.1% BSA, 2 mM $CaCl_2$, 2 mM MES, 10 mM KCl, 0.1% BSA, 1.5% cellulase, and 0.1% pectolyase, pH 5.5, and then incubated for 2 h at 22°C with gentle agitation. Protoplasts were collected through 70-μm cell strainers and concentrated by centrifugation at ~200*g*. The supernatant was aspirated and the cell pellet was resuspended in 10 mL of protoplast solution containing 600 mM mannitol, 2 mM $MgCl_2$, 0.1% BSA, 2 mM $CaCl_2$, 2 mM MES, 10 mM KCl, and 0.1% BSA, pH 5.5. Protoplasts were concentrated by centrifugation and then resuspended in 4 mL of protoplast solution. The protoplast suspension was then filtered through a 40-μm cell strainer.

Protoplasts expressing GFP were isolated using a fluorescence-activated cell sorter (FACSAria III; Becton Dickinson) fitted with a 130-μm nozzle. Protoplasts from non-GFP-expressing cells were used as a negative control. Protoplasts were sorted directly into RLT lysis buffer (Qiagen), mixed, and then immediately frozen at −80°C.

Quantitative Real-Time PCR Analysis

Total RNA was prepared from *Arabidopsis* cells using the SDS-phenol method, followed by DNase treatment and purification using an RNeasy plant mini kit (Qiagen) as described previously (Oda and Fukuda, 2011). After reverse transcription with the oligo(dT)20 primer and SuperScript III reverse transcriptase, quantitative real-time PCR was performed using a LightCycler (Roche Diagnostics) with LightCycler TaqMan Master Probes and universal Probe Library probes in combination with gene-specific primers designed by Probe Finder software (http://www.roche-applied-science.com). Quantitative real-time PCR analysis for the *UBIQUITIN10* gene was performed as a control. Quantification of gene expression was performed using LightCycler software, and the relative expression value compared with that of *UBIQUITIN10* was calculated. Data were average of three biological replicates.

Expression and Purification of Recombinant Proteins

The vectors were transformed into BL21 codon plus RIPL cells (Agilent). A single colony was picked and cultured at 37°C overnight in 2 mL of Luria-Bertani medium supplemented with carbenicillin. The starter culture was then transferred to 150 mL of Luria-Bertani medium and incubated at 28°C. When the OD_{600} of the culture reached 0.6, the temperature was reduced to 18°C and protein expression was induced using 0.5 mM isopropyl-β-D-thiogalactopyranoside. After 48 h of culture, cells were harvested by centrifugation and stored at −80°C.

To purify GST-Kif2A, GST-MIDD1, and GST-Kinesin-13A, cells were resuspended in HEM (10 mM HEPES, pH 7.4, 1 mM EGTA, and 1 mM $MgCl_2$) supplemented with 150 mM KCl, and lysates were prepared as described above. Glutathione-sepharose beads were added to the lysate and incubated for 30 min. Beads were washed three times with HEM supplemented with 100 mM KCl, and recombinant proteins were eluted with elution buffer comprising 100 mM HEPES, pH 7.4, 100 mM KCl, and 20 mM glutathione. A PD-10 column (GE Healthcare) was then used to change the buffer to BRB80 (80 mM PIPES, pH 6.9, 1 mM $MgCl_2$, and 1 mM EGTA) supplemented with 100 mM KCl. The eluted product was quantified by SDS-PAGE and Coomassie Brilliant Blue staining using BSA as a standard. The product was then divided into small aliquots, frozen in liquid nitrogen, and stored at −80°C.

Preparation of Taxol-Stabilized Microtubules

Porcine tubulin (10 mg/mL; Cytoskeleton) was incubated at 37°C for 15 min in BRB80 buffer containing 10 μM taxol and 1 mM DTT. Microtubules were pelleted by centrifugation at 22°C for 15 min at 100,000*g* and then resuspended in BRB80 buffer containing 50 mM KCl, 1 mM DTT, and 2 mM MgATP. For fluorescein labeling of microtubules, HiLyte 488-tagged porcine tubulin (Cytoskeleton) was mixed with porcine tubulin at a 1:9 ratio in BRB80 buffer, incubated in the presence of taxol and DTT, and then collected as described above.

Microtubule Depolymerizing Assay

Microtubule depolymerization was performed using taxol-stabilized microtubules. Assays were performed in 0.5× BRB80 supplemented with 50 mM KCl, 1 mM DTT, and either 2 mM MgATP or 2 mM AMPPNP. GST-Kif2A, GST-MIDD1, and GST-Kinesin-13A (each at 100 nM) were incubated with 1 μM microtubules. Protein mixtures were incubated for 15 min at 22°C and then centrifuged for 15 min at 22°C at 100,000*g*. The pellet was resuspended in BRB80 buffer, and the supernatant and resuspended pellets were analyzed by SDS-PAGE and Coomassie Brilliant Blue staining.

Accession Numbers

Sequence data from this article can be found in the GenBank/EMBL libraries under the following accession numbers: Kinesin-13A, AT3G16630; MIDD1, AT3G53350; ROP11, AT5G62880; TUB6, AT5G12250; and Kif2A, NM_004520.

Supplemental Data

The following materials are available in the online version of this article.

Supplemental Table 1. Primers Used in This Study.

Supplemental Movie 1. Dynamics of GFP-Kinesin-13A in the Cortex of Differentiating Xylem Cell.

ACKNOWLEDGMENTS

We thank Nobutaka Hirokawa (University of Tokyo) for providing the GST-Kif2A vector, Nam-Hai Chua (Rockefeller University) for providing the pER8 vector, Ueli Grossniklaus (University of Zurich) for providing the pMDC7 vector, and Tsuyoshi Nakagawa (Shimane University) for providing the pGWB vectors. We also thank Bo Liu (University of California) for helpful discussions and Yuki Nakashima (University of Tokyo) for technical assistance. This work was supported in part by Grants-in-Aid from the Ministry of Education, Science, Sports, and Culture of Japan to H.F. (19060009) and Y.O. (25114507), by the Japan Society for the Promotion of Science to H.F. (23227001) and Y.O. (25440128), by the Network of Centers of Carbon Dioxide Resource Studies in Plants project to HF, and by Japan Science and Technology Agency, Precursory Research for Embryonic Science and Technology to Y.O. (20103). This research was also supported in part by the Japan Advanced Plant Science Network.

AUTHOR CONTRIBUTIONS

Y.O. and H.F. wrote the article. Y.O. designed research and performed the experiments and data analysis.

Received August 29, 2013; revised October 22, 2013; accepted November 4, 2013; published November 26, 2013.

REFERENCES

Birnbaum, K., Jung, J.W., Wang, J.Y., Lambert, G.M., Hirst, J.A., Galbraith, D.W., and Benfey, P.N. (2005). Cell type-specific expression profiling in plants via cell sorting of protoplasts from fluorescent reporter lines. Nat. Methods **2:** 615–619.

Chan, J., Sambade, A., Calder, G., and Lloyd, C. (2009). *Arabidopsis* cortical microtubules are initiated along, as well as branching from, existing microtubules. Plant Cell **21:** 2298–2306.

Crowell, E.F., Bischoff, V., Desprez, T., Rolland, A., Stierhof, Y.D., Schumacher, K., Gonneau, M., Höfte, H., and Vernhettes, S. (2009). Pausing of Golgi bodies on microtubules regulates secretion of cellulose synthase complexes in *Arabidopsis*. Plant Cell **21:** 1141–1154.

Desai, A., Verma, S., Mitchison, T.J., and Walczak, C.E. (1999). Kin I kinesins are microtubule-destabilizing enzymes. Cell **96:** 69–78.

Dixit, R., and Cyr, R. (2004). Encounters between dynamic cortical microtubules promote ordering of the cortical array through angle-dependent modifications of microtubule behavior. Plant Cell **16:** 3274–3284.

Ems-McClung, S.C., and Walczak, C.E. (2010). Kinesin-13s in mitosis: Key players in the spatial and temporal organization of spindle microtubules. Semin. Cell Dev. Biol. **21:** 276–282.

Esau, K. (1977). Anatomy of Seed Plants, 2nd ed. (New York: Wiley).

Fu, Y., Gu, Y., Zheng, Z., Wasteneys, G., and Yang, Z. (2005). *Arabidopsis* interdigitating cell growth requires two antagonistic pathways with opposing action on cell morphogenesis. Cell **120:** 687–700.

Fu, Y., Xu, T., Zhu, L., Wen, M., and Yang, Z. (2009). A ROP GTPase signaling pathway controls cortical microtubule ordering and cell expansion in *Arabidopsis*. Curr. Biol. **19:** 1827–1832.

Fukuda, H. (2000). Programmed cell death of tracheary elements as a paradigm in plants. Plant Mol. Biol. **44:** 245–253.

Gutierrez, R., Lindeboom, J.J., Paredez, A.R., Emons, A.M., and Ehrhardt, D.W. (2009). *Arabidopsis* cortical microtubules position cellulose synthase delivery to the plasma membrane and interact with cellulose synthase trafficking compartments. Nat. Cell Biol. **11:** 797–806.

Homma, N., Takei, Y., Tanaka, Y., Nakata, T., Terada, S., Kikkawa, M., Noda, Y., and Hirokawa, N. (2003). Kinesin superfamily protein 2A (KIF2A) functions in suppression of collateral branch extension. Cell **114:** 229–239.

Lee, Y.R., and Liu, B. (2004). Cytoskeletal motors in Arabidopsis. Sixty-one kinesins and seventeen myosins. Plant Physiol. **136:** 3877–3883.

Li, S., Gu, Y., Yan, A., Lord, E., and Yang, Z.B. (2008). RIP1 (ROP Interactive Partner 1)/ICR1 marks pollen germination sites and may act in the ROP1 pathway in the control of polarized pollen growth. Mol. Plant **1:** 1021–1035.

Lin, D., Cao, L., Zhou, Z., Zhu, L., Ehrhardt, D., Yang, Z., and Fu, Y. (2013). Rho GTPase signaling activates microtubule severing to promote microtubule ordering in *Arabidopsis*. Curr. Biol. **23:** 290–297.

Lu, L., Lee, Y.R., Pan, R., Maloof, J.N., and Liu, B. (2005). An internal motor kinesin is associated with the Golgi apparatus and plays a role in trichome morphogenesis in *Arabidopsis*. Mol. Biol. Cell **16:** 811–823.

Maney, T., Wagenbach, M., and Wordeman, L. (2001). Molecular dissection of the microtubule depolymerizing activity of mitotic centromere-associated kinesin. J. Biol. Chem. **276:** 34753–34758.

Mao, G., Buschmann, H., Doonan, J.H., and Lloyd, C.W. (2006). The role of MAP65-1 in microtubule bundling during Zinnia tracheary element formation. J. Cell Sci. **119:** 753–758.

Mennella, V., Rogers, G.C., Rogers, S.L., Buster, D.W., Vale, R.D., and Sharp, D.J. (2005). Functionally distinct kinesin-13 family members cooperate to regulate microtubule dynamics during interphase. Nat. Cell Biol. **7:** 235–245.

Moores, C.A., and Milligan, R.A. (2006). Lucky 13-microtubule depolymerisation by kinesin-13 motors. J. Cell Sci. **119:** 3905–3913.

Mucha, E., Hoefle, C., Hückelhoven, R., and Berken, A. (2010). RIP3 and AtKinesin-13A - A novel interaction linking Rho proteins of plants to microtubules. Eur. J. Cell Biol. **89:** 906–916.

Murata, T., Sonobe, S., Baskin, T.I., Hyodo, S., Hasezawa, S., Nagata, T., Horio, T., and Hasebe, M. (2005). Microtubule-dependent microtubule nucleation based on recruitment of gamma-tubulin in higher plants. Nat. Cell Biol. **7:** 961–968.

Nakagawa, T., et al. (2007). Improved Gateway binary vectors: High-performance vectors for creation of fusion constructs in transgenic analysis of plants. Biosci. Biotechnol. Biochem. **71:** 2095–2100.

Nakamura, M., Ehrhardt, D.W., and Hashimoto, T. (2010). Microtubule and katanin-dependent dynamics of microtubule nucleation complexes in the acentrosomal *Arabidopsis* cortical array. Nat. Cell Biol. **12:** 1064–1070.

Noda, Y., Niwa, S., Homma, N., Fukuda, H., Imajo-Ohmi, S., and Hirokawa, N. (2012). Phosphatidylinositol 4-phosphate 5-kinase alpha (PIPKα) regulates neuronal microtubule depolymerase kinesin, KIF2A

and suppresses elongation of axon branches. Proc. Natl. Acad. Sci. USA **109:** 1725–1730.

Oda, Y., and Hasezawa, S. (2006). Cytoskeletal organization during xylem cell differentiation. J. Plant Res. **119:** 167–177.

Oda, Y., and Fukuda, H. (2011). Dynamics of *Arabidopsis* SUN proteins during mitosis and their involvement in nuclear shaping. Plant J. **66:** 629–641.

Oda, Y., and Fukuda, H. (2012a). Initiation of cell wall pattern by a Rho- and microtubule-driven symmetry breaking. Science **337:** 1333–1336.

Oda, Y., and Fukuda, H. (2012b). Secondary cell wall patterning during xylem differentiation. Curr. Opin. Plant Biol. **15:** 38–44.

Oda, Y., Iida, Y., Kondo, Y., and Fukuda, H. (2010). Wood cell-wall structure requires local 2D-microtubule disassembly by a novel plasma membrane-anchored protein. Curr. Biol. **20:** 1197–1202.

Oda, Y., Mimura, T., and Hasezawa, S. (2005). Regulation of secondary cell wall development by cortical microtubules during tracheary element differentiation in Arabidopsis cell suspensions. Plant Physiol. **137:** 1027–1036.

Ovechkina, Y., Wagenbach, M., and Wordeman, L. (2002). K-loop insertion restores microtubule depolymerizing activity of a "neckless" MCAK mutant. J. Cell Biol. **159:** 557–562.

Paredez, A.R., Somerville, C.R., and Ehrhardt, D.W. (2006). Visualization of cellulose synthase demonstrates functional association with microtubules. Science **312:** 1491–1495.

Pesquet, E., Korolev, A.V., Calder, G., and Lloyd, C.W. (2010). The microtubule-associated protein AtMAP70-5 regulates secondary wall patterning in *Arabidopsis* wood cells. Curr. Biol. **20:** 744–749.

Piao, T., Luo, M., Wang, L., Guo, Y., Li, D., Li, P., Snell, W.J., and Pan, J. (2009). A microtubule depolymerizing kinesin functions during both flagellar disassembly and flagellar assembly in Chlamydomonas. Proc. Natl. Acad. Sci. USA **106:** 4713–4718.

Shaw, S.L., Kamyar, R., and Ehrhardt, D.W. (2003). Sustained microtubule treadmilling in *Arabidopsis* cortical arrays. Science **300:** 1715–1718.

Stoppin-Mellet, V., Gaillard, J., and Vantard, M. (2006). Katanin's severing activity favors bundling of cortical microtubules in plants. Plant J. **46:** 1009–1017.

Van Bruaene, N., Joss, G., and Van Oostveldt, P. (2004). Reorganization and in vivo dynamics of microtubules during Arabidopsis root hair development. Plant Physiol. **136:** 3905–3919.

Wang, X., Zhang, J., Yuan, M., Ehrhardt, D.W., Wang, Z., and Mao, T. (2012). *Arabidopsis* microtubule destabilizing protein40 is involved in brassinosteroid regulation of hypocotyl elongation. Plant Cell **24:** 4012–4025.

Wang, X., Zhu, L., Liu, B., Wang, C., Jin, L., Zhao, Q., and Yuan, M. (2007). *Arabidopsis* MICROTUBULE-ASSOCIATED PROTEIN18 functions in directional cell growth by destabilizing cortical microtubules. Plant Cell **19:** 877–889.

Wasteneys, G.O., and Ambrose, J.C. (2009). Spatial organization of plant cortical microtubules: Close encounters of the 2D kind. Trends Cell Biol. **19:** 62–71.

Wei, L., Zhang, W., Liu, Z., and Li, Y. (2009). AtKinesin-13A is located on Golgi-associated vesicle and involved in vesicle formation/budding in *Arabidopsis* root-cap peripheral cells. BMC Plant Biol. **9:** 138.

Welburn, J.P., and Cheeseman, I.M. (2012). The microtubule-binding protein Cep170 promotes the targeting of the kinesin-13 depolymerase Kif2b to the mitotic spindle. Mol. Biol. Cell **23:** 4786–4795.

Winter, D., Vinegar, B., Nahal, H., Ammar, R., Wilson, G.V., and Provart, N.J. (2007). An "Electronic Fluorescent Pictograph" browser for exploring and analyzing large-scale biological data sets. PLoS ONE **2:** e718.

Xu, T., Wen, M., Nagawa, S., Fu, Y., Chen, J.G., Wu, M.J., Perrot-Rechenmann, C., Friml, J., Jones, A.M., and Yang, Z. (2010). Cell surface- and rho GTPase-based auxin signaling controls cellular interdigitation in Arabidopsis. Cell **143:** 99–110.

Yang, Z. (2008). Cell polarity signaling in *Arabidopsis*. Annu. Rev. Cell Dev. Biol. **24:** 551–575.